GPS Solut (2013) 17:347–355
DOI 10.1007/s10291-012-0283-7

ORIGINAL ARTICLE

Fast estimation and analysis of the inter-frequency clock bias for Block IIF satellites

Haojun Li · Xuhua Zhou · Bin Wu

Received: 28 April 2012 / Accepted: 26 July 2012 / Published online: 15 August 2012

Abstract The inter-frequency bias of PRN25 was noticed by the scientific community and considered to be caused by thermal variations. The inter-frequency bias leads to an apparent inter-frequency clock bias (IFCB), which could be obtained using the difference of two ionosphere-free phase combinations (L1/L2 and L1/L5). We present an efficient approach derived from the epoch-differenced strategy for fast estimation of IFCBs for Block IIF satellites. For the analysis, data from 32 stations from the IGS network spanning 10 months (DOY 213, 2011–153, 2012) are processed. The processing times show that the epoch-differenced method is more efficient than the undifferenced one. In order to study the features of IFCB, a harmonic analysis is performed by using a FFT (fast Fourier transformation), and significant periodic variations with the periods of 12, 6 and 8 h are noticed. The fourth-order period is determined by comparing the performances of the model with different periods. After determination, a harmonics-based function of order 4 is used to model the IFCB, and the single-day amplitudes and phases are estimated for the 10 months from a least squares fit. Based on the estimated results, the characterization of IFCB is discussed. The algorithm is incorporated into the MGPSS software developed at SHAO (Shanghai Astronomical Observatory, Chinese Academy of Sciences) and used to monitor the IFCB variations of GPS and COMPASS systems in near real time.

H. Li (✉) · X. Zhou · B. Wu
Shanghai Astronomical Observatory, Chinese Academy of Sciences, Shanghai 200030, People's Republic of China
e-mail: yanlhjch@126.com

H. Li · B. Wu
Shanghai Key Laboratory of Space Navigation and Position Techniques, Shanghai 200030, People's Republic of China

Keywords Triple-frequency signals · Precise point positioning · Inter-frequency clock bias

Introduction

The Chinese COMPASS system, the modernized GPS satellites, the European Galileo system and the Japanese Quasi-Zenith Satellite System (QZSS) provide signals on three or more carrier frequencies. Some studies are carried out by using the real triple-frequency data (Hauschild et al. 2012a, b; Montenbruck et al. 2011a, b). An apparent inconsistency between three frequency carrier phases in the GPS systems was noted by the scientific community, which was understood to be caused a thermally dependent inter-frequency bias (Montenbruck et al. 2011a, b). The inter-frequency bias (IFB) of QZSS signal also is investigated by using the real data of the first QZSS satellite. The results show that there is no IFB variation in QZSS triple-frequency signals (Hauschild et al. 2012a).

In the current clock estimations (Hauschild and Montenbruck 2009; Bock et al. 2009; Ge et al. 2012; Li et al. 2010a, b), L1/L2-based ionosphere-free linear combination is normally used, and the impacts of IFBs exist in satellite clocks. Consequently, the satellite clocks derived from L1/L2 phase observations cannot be used for L1/L5-based precise point positioning (PPP) (Zumberge et al. 1997) without careful consideration of these biases. To enable a consistent use of L1/L2 clock products in L1/L5-based positioning and contribute to a better clock predictability at timescales of several hours, the inter-frequency clock bias (IFCB) of PRN25 has been estimated by using the undifferenced approach in Montenbruck et al. (2011a, b). With the developments of all the systems, the estimation of the satellite clock offset will be carried out as a routine

service. For the estimation of IFCBs, undifferenced phase observations of a global network are normally used. This involves the estimation of a large number of ambiguities and epoch-wise bias parameters. The computation is time consuming.

To improve the computation efficiency, a new method derived from the epoch-differenced (ED) approach (Ge et al. 2012; Li et al. 2010a, b, 2012) is introduced for IFCB estimation. In order to evaluate the method presented and to study the features of the IFCBs, data from 32 stations from the IGS network spanning 10 months (DOY 213, 2011–153, 2012) are processed. Based on the estimated results, a spectrum analysis is performed by using a FFT (fast Fourier transformation), and the features of PRN01 and PRN25 are studied. The processing times of the undifferenced and ED approaches are compared to validate the computational efficiency. In the following, "Estimation" section introduces estimation approaches. "Empirical model" section introduces the model of IFCBs. "Data processing" section presents the data analysis and discusses the results. Finally, "Conclusions and discussions" section summarizes the main findings.

Estimation

The IFCB has been estimated in a general strategy (Montenbruck et al. 2011a, b). However, such strategy is time consuming and a complicated handling of ambiguities is needed. To reduce the computational burden, we introduce a computationally efficient approach for fast IFCB estimation here. The presented approach removes the ambiguity parameters, and only ED IFCBs remain. Selecting a reference epoch and setting a referenced IFCB, the reference epoch-based IFCB is then computed using the estimated ED IFCB.

Undifferenced approach

The geometric range and tropospheric delay can be removed by differencing two different ionosphere-free measurements (L1/L2 and L1/L5), and the remaining terms are ambiguity and inter-frequency clock biases. The differenced ionosphere-free measurement (DIF) is given by (Montenbruck et al. 2011a):

$$\begin{aligned}\mathrm{DIF}(L_1,L_2,L_5) &= \mathrm{IF}(L_1,L_2) - \mathrm{IF}(L_1,L_5)\\ &= (\delta_{1,2}-\delta_{1,5}) + const_3 - const_6\end{aligned} \quad (1)$$

where $const_3$ is the ambiguity of ionosphere-free combination formed with L1 and L2, $const_6$ is the ambiguity of ionosphere-free combination formed with L1 and L5, and the term $\delta_{1,2}$–$\delta_{1,5}$ is the inter-frequency clock bias (IFCB) between the L1/L2 and L1/L5 combinations. Based on (1), the IFCB could be estimated in a general clock estimation procedure (Montenbruck et al. 2011a, b).

Differenced approach

From (1) we have:

$$\begin{aligned}\delta &= \delta_{1,2} - \delta_{1,5}\\ &= \mathrm{DIF}(L_1,L_2,L_5) - const_3 + const_6\end{aligned} \quad (2)$$

where δ is the IFCB. Assuming there is no cycle slip between two adjacent epochs, the ambiguity term in (2) can be eliminated by differencing the DIF phase measurement at epoch m and $m-1$. We can obtain:

$$\begin{aligned}\Delta\delta(m) &= (\delta_{1,2}-\delta_{1,5})(m)\\ &= \mathrm{DIF}(L_1,L_2,L_5)(m) - \mathrm{DIF}(L_1,L_2,L_5)(m-1)\end{aligned} \quad (3)$$

where "Δ" indicates the ED operator, and $\Delta\delta$ is the ED IFCB. Assuming there are n stations in the network, which improves the redundancy of the solution, the ED IFCB $\Delta\delta(m)$ can be calculated by averaging $\Delta\delta(m)_k$ over the entire network:

$$\Delta\delta(m) = \frac{1}{n}\cdot\sum_{k=1}^{n}\Delta\delta(m)_k \quad (4)$$

Using the estimated ED IFCBs and the IFCB at a selected reference epoch, the reference epoch-based IFCB at epoch m can be expressed as:

$$\delta(m) = \delta(m_0) + \sum_{j=m_0+1}^{m}\Delta\delta(j) \quad (5)$$

where $\delta(m_0)$ is the IFCB at the reference epoch m_0, $\Delta\delta(j)$ is the ED IFCB at epoch j, and m is the number of epochs between the reference epoch m_0 and epoch m.

Empirical model

In order to describe the IFCB and study its features, two models are introduced. One is a sun-earth-satellite (SES) angle α-based simple model, and the other is a high-order harmonics-based model that is similar to the model shown in Montenbruck et al. (2011a).

SES angle α-based simple model

The IFCB is considered to depend on the periodic surface temperature changes of the Block IIF satellites through analyzing the results of PRN25 (Montenbruck et al. 2011a, b). In order to describe the state of the satellite and the relationship between the sun, earth and satellite, the angle α (Fig. 1) is used.

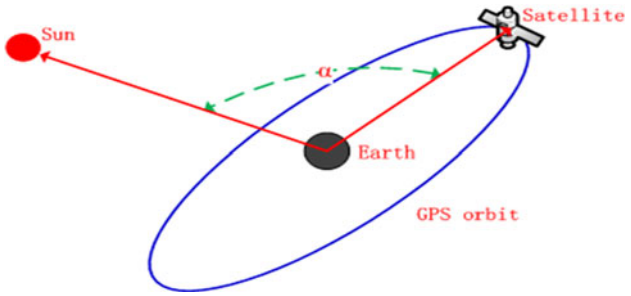

Fig. 1 Geometrical relationship between the sun, earth and satellite and definition of the SES angle α

Although the IFCB of PRN25 is modeled using a high-order harmonics-based composite function (Montenbruck et al. 2011a), a new simple model is still presented here. We assume that the simple model can describe the IFCB well if the sun illumination is the only factor caused IFCB. In other words, the performance of the simple model can test the theory of the sun illumination stated in Montenbruck et al. (2011a). Based on the computed sinusoidal values, the approximate expressions for the harmonic coefficients in terms of α have been established for the IFCBs. We model the IFCB using the following simple formula constructed by a sinusoidal function of α and a linear function:

$$\delta(t) = c + b \cdot t + \lambda \cdot \sin(\alpha + \theta),\ (\alpha = f(t), t = 0 \sim 24\,\mathrm{h}) \tag{6}$$

where c is a constant offset reflecting the offset between the sinusoidal function and true IFCBs, b is the linear term, t is the observation time, θ is phase offset, and λ is amplitude.

High-order harmonics-based model

Similar to the model shown in Montenbruck et al. (2011a), a high-order harmonics-based model is used to describe the IFCBs of the PRN25 and PRN01. The model is written as:

$$\delta(t) = c + b \cdot t + \sum_{i=1}^{4} \lambda_i \cdot \sin\left(\frac{2\pi}{T_i} \cdot t + \theta_i\right),\ (t = 0 \sim 24\,\mathrm{h}) \tag{7}$$

where i is the order of the harmonics, T_i is the period, θ_i is phase offset, and λ_i is the amplitude.

Data processing

To validate the approach presented and to study the features of the IFCB, the 10-month (DOY 213, 2011–153, 2012) data from 32 stations from the IGS network (Dow et al. 2005) are processed. Data are sampled at 30 s, and the data of PRN01 are used from DOY 277, 2011 as it was set healthy since then. Figure 2 shows the distribution of the 32 stations, which have the capability to track the new L5 signal of the Block IIF satellites. Data processing is performed on a Windows personal computer with Intel (R) Dual Core(TM) 2.4-HZ processor and 2-GB memory.

Processing time

Table 1 shows the average processing time for 1 day of data in the ED and undifferenced approaches. The table

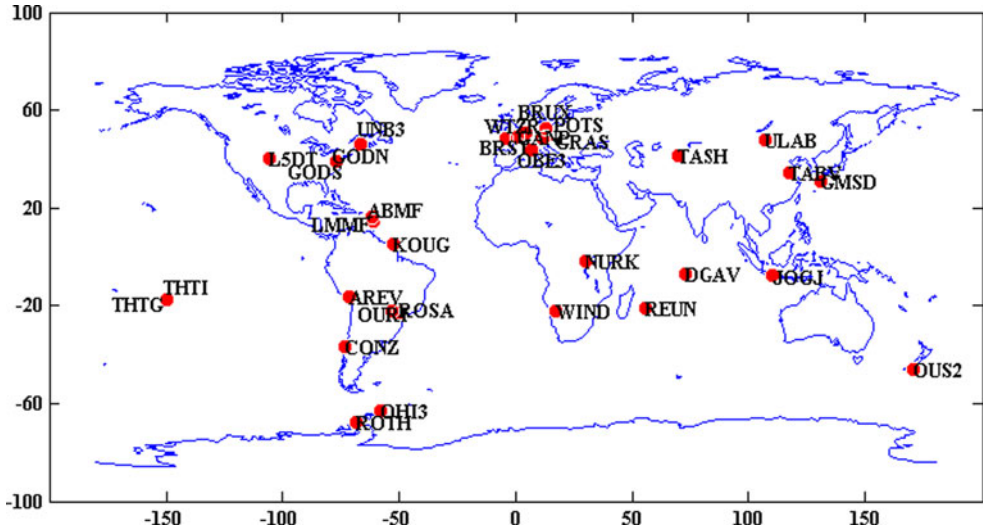

Fig. 2 Distribution of the 32 IGS stations tracking the GPS L5 signal

Table 1 Total processing time for 1 day of data and average processing time per epoch for undifferenced and ED approaches

Approach	ED	Undifferenced
Total time (s)	289	434
Time per epoch (s)	0.10	0.15

illustrates that the ED approach is able to process 9–10 epochs within 1 s, and it is almost 1.5 times faster than the undifferenced one. It shows that the ED approach is much more efficient, especially for real-time applications.

Period

It is important to determine the periods of all orders for describing the IFCB with high-order harmonics-based composite function. In this contribution, a harmonic analysis is performed by using a FFT based on the 10-month single-day-estimated IFCBs of PRN25 and PRN01. The 10-month single-day periods (T_i ($i = 1 \sim 4$)) of each satellite are illustrated in Fig. 3. The figure indicates that the PRN25 and PRN01 have notable periodic variations with periods of 12, 6 and 8 h. Based on the sun illumination and thermal consideration stated in Montenbruck et al. (2011a), the 12-h period can be explained as much as the satellite takes in the same sun illumination, before and after 12 h, because the direction and position of the satellite are approximately equal at two time points. Likewise, the 6-h period can be understood in that the two positions of the satellite, before and after 6 h, have the equal heat. The 8-h period cannot be explained by sun illumination, which indicates that other factors may affect the satellite clock or signals. All factors including the sun illumination cause the real IFCB. Unfortunately, it is difficult to gain further information about the internal and external satellite properties to identify what other factors are involved. The determination of the fourth-order period is discussed in the next section by comparing the performances of the different groups of period.

Performance of the model

The coefficients (c, b, θ and λ) of the simple model are estimated from a least squares fit for a 24-h data arc over the 10 months. Inserting the estimated coefficients into (6), the modeled values of the IFCB are obtained. Comparing the modeled IFCBs with estimated ones, the 10-month single-day RMSs are computed and illustrated in Fig. 4. To further study the performance of the model, the correctional rate is defined and given by:

$$P = (1 - \mathrm{RMS_D}/\mathrm{RMS_E}) \cdot 100\,\% \tag{8}$$

where P is the correctional rate, $\mathrm{RMS_D}$ is the RMS of the difference between the modeled and estimated IFCB, $\mathrm{RMS_E}$ is the RMS of the estimated IFCB. The correctional rates of the simple model are computed and illustrated in Fig. 5. The RMS values and the correctional rates in Figs. 4 and 5 indicate the simple model can only correct 47.2 and 45.5 % IFCBs of PRN01 and PRN25, respectively. There remain contributions of high-order terms after the IFCB is corrected using the simple model. The performance of the simple mode further validates that other factors may exist that disturb the satellite clock or signals besides sun illumination.

It is understood that the high-order harmonics-based function can well describe the IFCB and GPS clock, especially the fourth-order harmonics-based function (Senior et al. 2008; Montenbruck et al. 2011a). "Period" section shows that the IFCBs of PRN25 and PRN01 have apparent periods of 12, 6 and 8 h, but their fourth-order period is indistinct. The final products of IGS are used to analyze the characterization of period variation in GPS clock (Senior et al. 2008). The 12-, 6-, 4- and 3-h periods are noticed. Based on those considerations, different groups of period are used to model the IFCBs. The harmonic coefficients (θ_i ($i = 1 \sim 4$) and λ_i ($i = 1 \sim 4$)) of different groups are estimated from a least squares fit for a 24-h data arc over the 10 months. Inserting the estimated coefficients and used periods into (7), the modeled IFCBs are obtained. Comparing the modeled IFCBs with estimated ones, the RMSs and correctional rates of different

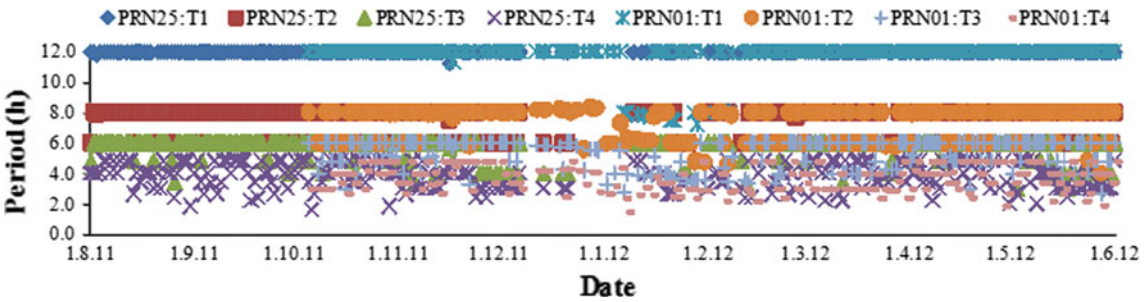

Fig. 3 Periods of the single-day IFCB for PRN01 and PRN25, for the time DOY 213, 2011–153, 2012. The axis is labeled DD.MM.YY

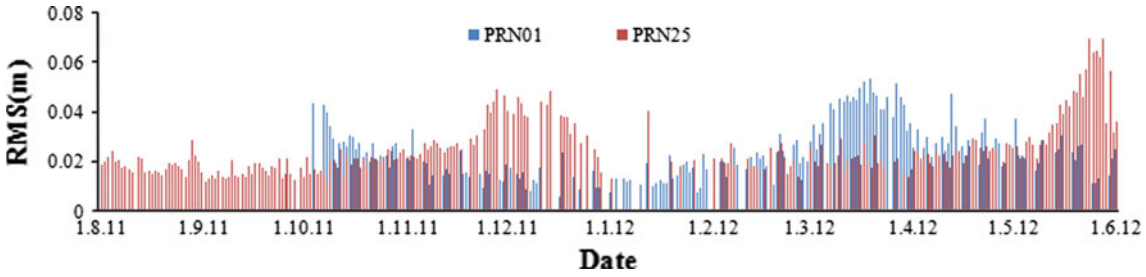

Fig. 4 RMS for the simple model compared with the estimated ones

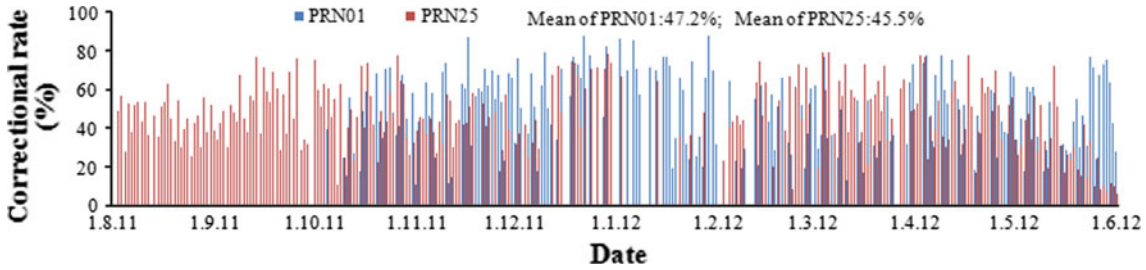

Fig. 5 Correctional rates of the simple model

groups are computed. The means of the 10-month single-day correctional rates of different groups are shown in Table 2. The table reveals that the fourth-order harmonics-based model with the periods of 12, 6, 8 and 4 h is better than others. From the IFCBs of DOY 308, 2011 in Fig. 6, it is observed that the modeled and estimated IFCBs are quite consistent, which further validates the appropriateness of the periods (T_i $(i = 1 \sim 4)$) of 12, 6, 8 and 4 h. The 10-month single-day RMSs of the model with the periods of 12, 6, 8 and 4 are illustrated in Fig. 7. The figure shows that the fourth-order harmonics-based model with the periods of 12, 6, 8 and 4 h can reach millimeter level in most cases. From Fig. 5 and Table 2, it can be seen that the simple model can reach more than 50 % accuracy of the fourth-order harmonics-based model.

Amplitude

Based on the performances of the model with the periods (T_i $(i = 1 \sim 4)$) of 12, 6, 8 and 4 h, its amplitudes and phases are selected to study the features of the IFCBs. The 10-month single-day amplitudes (λ_i $(i = 1 \sim 4)$) of PRN01 and PRN25 are illustrated in Figs. 8 and 9, respectively. These figures show that the variations of the amplitude with periods of 12 and 6 h of each satellite behave similarly. Comparing the amplitudes with period of 8 h with that of other ones, its variations are much slower, even as the satellites approach and enter the eclipse phases. Considering the increased IFCB variations during the eclipse phase (Montenbruck et al. 2011a), it is noted that the eclipse phase is encountered by the PRN01 in March 2012, while the PRN25 encountered it in December and June 2012, respectively. There is a difference between the eclipse phases of PRN01 and PRN25, and the difference is about 3 months. Combined with the results of the eclipse phases of PRN25 stated in Montenbruck et al. (2011a), the period of the eclipse phase of PRN25 is obtained and is about 6 months. From Figs. 4, 5, 8 and 9, it is obviously observed that the performances of the simple model become worse, when the satellites approach and enter the eclipse phases.

Table 2 Group of period, mean of the correctional rate

Group of period	Mean of correctional rate (percentage)	
	PRN01	PRN25
$T_1 = 12$ h, $T_2 = 6$ h, $T_3 = 8$ h	75.1	75.7
$T_1 = 12$ h, $T_2 = 6$ h, $T_3 = 8$ h, $T_4 = 4$ h	77.1	77.9
$T_1 = 12$ h, $T_2 = 6$ h, $T_3 = 8$ h, $T_4 = 3$ h	75.8	76.4
$T_1 = 12$ h, $T_2 = 6$ h, $T_3 = 4$ h, $T_4 = 3$ h	74.2	75.5

The amplitude series is fitted by using the following quadratic function:

$$\lambda_i(t_1)(i = 1 \sim 4) = a_0 + a_1 \cdot t_1 + a_2 \cdot t_1^2 \quad (9)$$

where a_0 is a constant, a_1 is the velocity of the amplitude variation, a_2 is the acceleration of the amplitude variation, t_1 is the time, and its unit is day. The RMSs of the fitted amplitudes compared with estimated ones are computed and shown in Table 3. The RMS values reveal that the quadratic function can well describe the variation of amplitude and have an accuracy of millimeter level, which

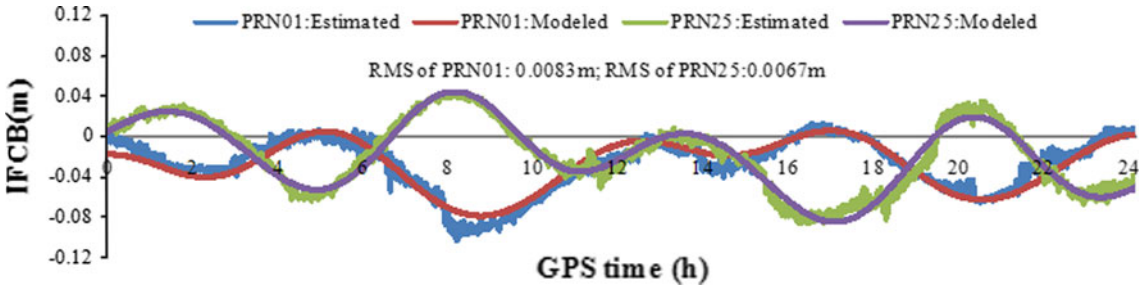

Fig. 6 Estimated and modeled IFCBs, DOY 308, 2011

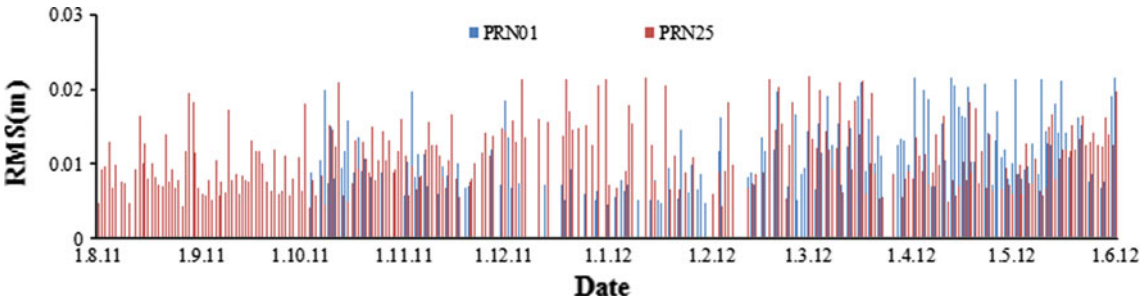

Fig. 7 RMSs of the modeled IFCBs compared with the estimated ones

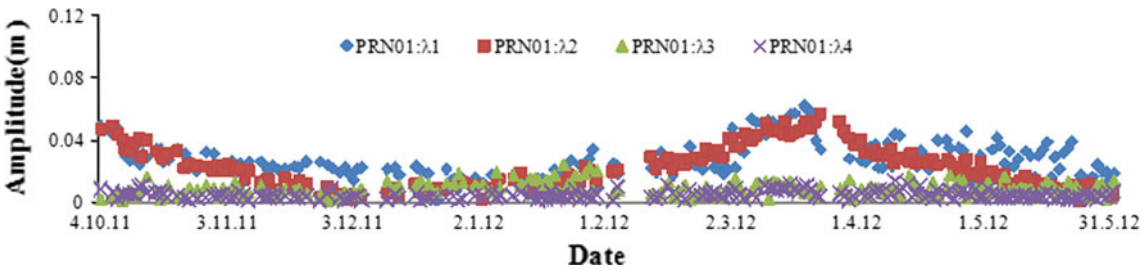

Fig. 8 Amplitudes of PRN01 for DOY 277, 2011–153, 2012

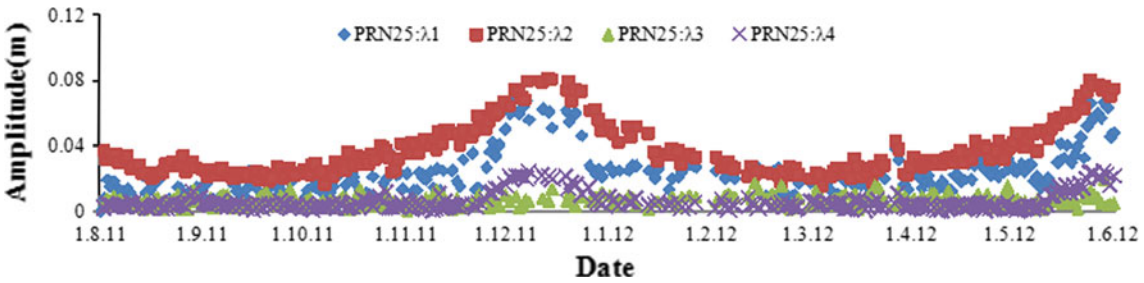

Fig. 9 Amplitudes of PRN25 for DOY 213, 2011–153, 2012

demonstrates that the amplitudes can be predicted using the quadratic function.

Phase

The 10-month single-day phases (θ_i $(i = 1 \sim 4)$) of PRN01 and PRN25 are illustrated in Figs. 10 and 11, respectively. The figures show that the phases of the 12- and 6-h periods have the characterization of linear variation, especially the phase of the 6-h period. The characterization can contribute to a better phase predictability at timescales of several days. The single-day 24-h IFCBs are modeled using (7). The main contribution to phase velocity is considered to be caused by the difference

Table 3 RMS of fitted amplitudes with respect to estimated ones; the unit is centimeter

Satellite	RMS			
	λ_1	λ_2	λ_3	λ_4
PRN01	0.79	0.37	0.39	0.21
PRN25	0.78	0.45	0.36	0.31

Table 4 Fitted phase velocity; the unit is degrees per day

Satellite	Period (h)	Phase velocity (b_1)	Mean
PRN01	12	2.11	2.24
	6	2.36	
PRN25	12	1.84	1.90
	6	1.95	

between the orbital period and the 24-h span of the modeled IFCBs. The difference accumulates over time causing the liner variation of phase. The phase velocity can be computed based on the orbital period. The formula is written as:

$$b_1 = 2 \cdot (360/T') \cdot (12 - T') \tag{10}$$

where b_1 is the phase velocity, and T' is the orbital period. The reported mean GPS orbital period is 11.9659 ± 0.0007 h. Submitting the mean orbital period into (10), the phase velocity of the periods of 6 and 12 h is obtained, and its value is 2.05 degrees per day.

The phase series of the 12- and 6-h periods is fitted by the linear function as follows:

$$\theta_i(t_1)(i = 1 \sim 4) = b_0 + b_1 \cdot t_1 \tag{11}$$

where b_0 is a constant, and b_1 is the phase velocity. The fitted results are shown in Table 4.

Comparing the fitted and computed phase velocities, the differences between two sets of phase velocities are obtained. The differences of PRN01 and PRN25 are 0.19 and 0.15 degrees per day, respectively. The approximate two sets of phase velocities validate the rationality about the interpretation of the linear variation of the phase. The computation of the orbital period of satellite can be implemented by using the fitted phase velocity. The computed orbital periods of PRN01 and PRN25 are 11.9628 h and 11.9684 h, respectively. The computed orbital periods are approximation of the reported mean GPS orbital period of 11.9659 ± 0.0007 h.

Conclusions and discussions

A new approach for fast IFCB estimation has been developed. Using the data from 32 stations spanning 10 months, the IFCBs for Block IIF satellites PRN01 and PRN25 are investigated. The processing times of the undifferenced and ED approaches indicate that the presented approach is more efficient than the traditional absolute IFCB estimation strategy.

Similar to the PRN25, the PRN01 has also apparent IFCB variations. The notable periods of 12, 6 and 8 h of the single-day IFCB are noticed by performing a harmonic analysis. The fourth-order period of 4 h is determined by comparing the performances of the different groups of period. After determination, a fourth-order harmonics-

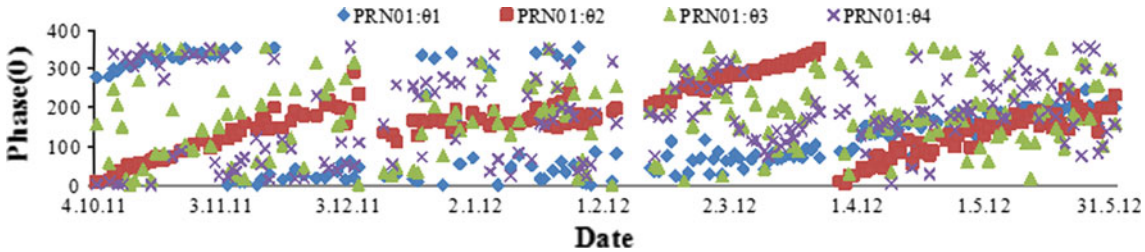

Fig. 10 Phases of PRN01 for DOY 277, 2011–153, 2012

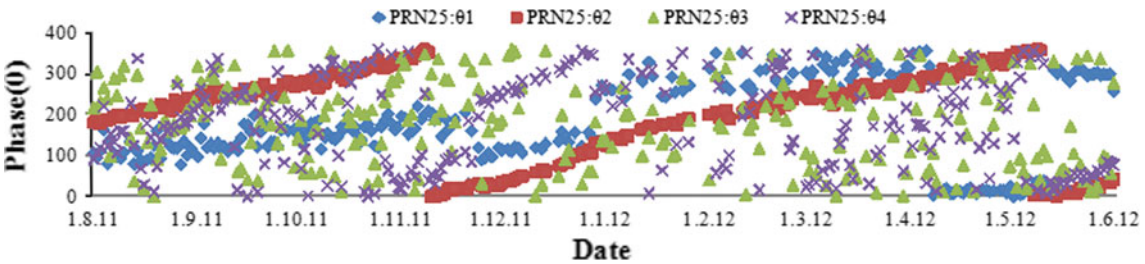

Fig. 11 Phases of PRN25 for DOY 213, 2011–153, 2012

based model with the periods of 12, 6, 8 and 4 h is selected to describe the IFCB. The correctional rates indicate the simple model can only correct 47.2 and 45.5 % IFCBs of PRN01 and PRN25, respectively, while the model with the periods of 12, 6, 8 and 4 h can correct 77.1 and 77.9 % IFCBs. The performance of the simple model and the 8-h period reveals that other factors come into play besides the sun illumination and disturb the signal or clock. The RMSs show that the simple model is sensitive to the eclipse phase. Its performance becomes worse, when the satellites approach and enter the eclipse phase.

The amplitudes and phases of PRN01 and PRN25 are estimated using the selected fourth-order model. The estimated results show that the amplitudes have the characterization of quadratic curve, while the phases have the characterization of linear variation. The characterizations can contribute to the better amplitude and phase predictability at timescales of several days. Amplitude analysis shows that the PRN01 and PRN25 have different eclipse phases. The difference between the two eclipse phases of PRN01 and PRN25 is about 3 months. Combined with the results in Montenbruck et al. (2011a), the period of the eclipse phase of PRN25 is obtained and is about 6 months. The direct and inverse computation can be implemented between the phase velocity and the orbital period, which can be used to monitor each other.

Acknowledgments This research is supported by the National Natural Science Foundation of China (NSFC) (No: 11173049 and 41174023) and the Opening Project of Shanghai Key Laboratory of Space Navigation and Position Techniques (No: Y224353002). IGS is acknowledged for providing RINEX data. Professor Oliver Montenbruck is acknowledged for his valuable comments. The authors are also grateful for the comments by the editor and two reviewers, which helped us to improve our manuscript significantly.

References

Bock H, Dach R, Jäggi A, Beutler G (2009) High-rate GPS clock corrections from CODE: support of 1 Hz applications. J Geod 83(11):1083–1094. doi:10.1007/s00190-009-0326-1

Dow J, Neilan R, Gendt G (2005) The International GPS Service: celebrating the 10th anniversary and looking to the next decade. Adv Space Res 36(3):320–326. doi:10.1016/j.asr.2005.05.125

Ge M, Chen J, Dousa J, Gendt G, Wickert J (2012) A computationally efficient approach for estimating high-rate satellite clock corrections in realtime. GPS Solut 16:9–17. doi:10.1007/s10291-011-0206-z

Hauschild A, Montenbruck O (2009) Kalman-filter-based GPS clock estimation for near realtime positioning. GPS Solut 13:173–182. doi:10.1007/s10291-008-0110-3

Hauschild A, Steigenberger P, Rodriguez-Solano C (2012a) Signal, orbit and attitude analysis of Japan's first QZSS satellite Michibiki. GPS Solut 16:127–133. doi:10.1007/s10291-011-0245-5

Hauschild A, Montenbruck O, Sleewaegen J, Huisman L, Teunissen P (2012b) Characterization of compass M-1 signals. GPS Solut 16:117–126. doi:10.1007/s10291-011-0210-3

Li H, Chen J, Wang J, Hu C, Liu Z (2010a) Network based real-time precise point positioning. Adv Space Res 46(9):1218–1224. doi:10.1016/j.asr.2010.06.015

Li H, Wang J, Chen J, Hu C, Wang H (2010b) The realization and analysis of GNSS network based real-time precise point positioning. Chin J Geophys 53(6):1302–1307. doi:10.3969/j.issn.0001-5733.2010.06.008

Li H, Chen J, Wang J, Wu B (2012) Satellite- and epoch differenced precise point positioning based on regional augmentation network. Sensors 12(6):7518–7528. doi:10.3390/s120607518

Montenbruck O, Hugentobler U, Dach R, Steigenberger P, Hauschild A (2011a) Apparent clock variations of the Block IIF-1 (SVN62) GPS satellite. GPS Solut. doi:10.1007/s1029 1-011-0232-x

Montenbruck O, Steigenberger P, Schönemann E, Hauschild A, Hugentobler U, Dach R, Becker M (2011b) Flight characterization of new generation GNSS satellite clocks. ION-GNSS-2011, 21–23 Sep 2011, Portland OR, USA

Senior K, Ray J, Beard R (2008) Characterization of periodic variations in the GPS satellite clocks. GPS Solut 12(3):211–225. doi:10.1007/s10291-008-0089-9

Zumberge JF, Heflin MB, Jefferson DC, Watkins MM, Webb FH (1997) Precise point positioning for the efficient and robust analysis of GPS data from large networks. J Geophys Res 102(3):5005–5017. doi:10.1029/96JB03860

Author Biographies

Haojun Li received his PhD in Geodesy at the Tongji University, Shanghai, China. He is a research assistant at Shanghai Astronomical Observatory (SHAO), Chinese Academy of Sciences. His main research interests include precise point positioning, satellite clock estimation and multi-frequency GNSS.

Xuhua Zhou is a professor at Astronomical Observatory, Chinese Academy of Sciences. His main research field includes precise orbit determination, satellite altimetry and gravity, tides.

Bin Wu is a professor and a director of the Center for Astro-geodynamics Research, Shanghai Astronomical Observatory. His main research fields include GNSS and SLR system and their applications for geodesy, precise orbit determination, earth rotation and reference frames.